

# Spin-Valleytronics in Silicene: Quantum-Spin-Quantum-Anomalous Hall Insulators and Single-Valley Semimetals

Motohiko Ezawa

Department of Applied Physics, University of Tokyo, Hongo 7-3-1, 113-8656, Japan

Valley-based electronics, known as valleytronics, is one of the keys to break through to a new stage of electronics. The valley degree of freedom is ubiquitous in the honeycomb lattice system. The honeycomb lattice structure of silicon called silicene is an fascinating playground of valleytronics. We investigate topological phases of silicene by introducing different exchange fields on the  $A$  and  $B$  sites. There emerges a rich variety of topologically protected states each of which has a characteristic spin-valley structure. The single Dirac-cone semimetal is such a state that one gap is closed while the other three gaps are open, evading the Nielsen-Ninomiya fermion-doubling problem. We have newly discovered a hybrid topological insulator named the quantum-spin-quantum-anomalous Hall insulator, where the quantum anomalous Hall effect occurs at one valley and the quantum spin Hall effect occurs at the other valley. Along its phase boundary, single-valley semimetals emerge, where only one of the two valleys is gapless with degenerated spins. These semimetals are also topologically protected because they appear in the interface of different topological insulators. Such a spin-valley dependent physics will be observed by optical absorption or edge modes.

**Introduction:** The intrinsic degrees of freedom of an electron are its charge and spin, which lead to electronics and spintronics. The valley degree of freedom on honeycomb lattices is expected to provide us with the notion of valleytronics. Valleytronics was originally proposed in graphene[1–3], where the states near the Fermi energy are  $\pi$  orbitals residing near the  $K$  and  $K'$  points at opposite corners of the hexagonal Brillouin zone. The low-energy dynamics in the  $K$  and  $K'$  valleys is described by the Dirac theory. The valley excitations are protected by the suppression of intervalley scattering. However it is hard to realize valleytronics in graphene since the gap is closed and since it is difficult to discriminate between the  $K$  and  $K'$  points experimentally. In this context, transition metal dichalcogenides[4–7] become a new playground of valleytronics, where a considerably large gap is open. In the most recent experimental progress, the identity of valleys manifests as valley-selective circular dichroism, leading to valley polarization with circularly polarized light, offering a possibility to a realization of valleytronics[3–7].

Recently, another honeycomb system of silicon named silicene has been experimentally synthesized[8–10] and theoretically explored[11–14]. It consists of buckled sublattices made of  $A$  sites and  $B$  sites. Controlling the gap at the  $K$  and  $K'$  points independently by applying external fields such that electric field[12], photo-irradiation[13] and exchange field[14], we are able to generate a rich variety of topologically protected states in silicene, each of which has a characteristic spin-valley structure.

Well-known topologically protected states are quantum spin Hall (QSH)[15] and quantum anomalous Hall (QAH) insulators[16–21]. They are characterized by the helical and chiral gapless edge modes, respectively, when nanoribbons are made[22–24]. The QAH effect is the quantum Hall effect without Landau levels, while the QSH effect is the quantum Hall effect of spins rather than charges.

In this paper, to search for a full control of the valley degree of freedom, we make the use of the silicene's buckled

structure and introduce different exchange fields  $M_A$  and  $M_B$  operating on the  $A$  and  $B$  sites. This could be realized by attaching ferromagnets to silicene from the front and back sides. We obtain rich phase diagrams as illustrated in Fig.1 and Fig.3. First of all, we are able to generate the spin-polarized QAH (SQAH) insulator together with single Dirac-cone (SDC) semimetals along its phase boundaries [Fig.2]. The SDC semimetal is a remarkable state that has one massless Dirac cone and three massive Dirac cones, evading the Nielsen-Ninomiya fermion-doubling problem[25]. Second, a new finding is the quantum-spin-quantum-anomalous Hall (QSQAH) insulator. It is a new type of topological insulator such that, e.g., the QAH effect is realized at the  $K$  point while the QSH effect is realized at the  $K'$  point [Fig.4]. Third, another new finding is a single-valley (SV) semimetal such that, e.g., the gap is open (closed) at the  $K$  ( $K'$ ) point with spin degeneracy. It is different from the SDC state which has only one closed gap without spin degeneracy. These valley dependent band structures will be experimentally observed by spin-valley selective circular dichroism. In what follows we use notations  $s_z = \uparrow, \downarrow$ ,  $t_z = A, B$ ,  $\eta = K, K'$  in indices while  $s_z = \pm 1$ ,  $t_z = \pm 1$ ,  $\eta = \pm 1$  in equations for the spin, the sublattice pseudospin and the valley, respectively.

**Hamiltonian:** Silicene is described by the four-band second-nearest-neighbor tight binding model[12, 14, 26],

$$\begin{aligned}
 H = & -t \sum_{\langle i,j \rangle \alpha} c_{i\alpha}^\dagger c_{j\alpha} + i \frac{\lambda_{\text{SO}}}{3\sqrt{3}} \sum_{\langle\langle i,j \rangle\rangle \alpha\beta} \nu_{ij} c_{i\alpha}^\dagger \sigma_{\alpha\beta}^z c_{j\beta} \\
 & - i \frac{2}{3} \lambda_{\text{R2}} \sum_{\langle\langle i,j \rangle\rangle \alpha\beta} t_z^i c_{i\alpha}^\dagger \left( \boldsymbol{\sigma} \times \hat{\mathbf{d}}_{ij} \right)_{\alpha\beta}^z c_{j\beta} \\
 & - \ell \sum_{i\alpha} t_z^i E_z c_{i\alpha}^\dagger c_{i\alpha} + \sum_{i\alpha} M_{t_z} c_{i\alpha}^\dagger \sigma_z c_{i\alpha}, \quad (1)
 \end{aligned}$$

where  $c_{i\alpha}^\dagger$  creates an electron with spin polarization  $\alpha$  at site  $i$ , and  $\langle i, j \rangle$  ( $\langle\langle i, j \rangle\rangle$ ) run over all the nearest (next-nearest-

neighbor) hopping sites. We explain each term. (i) The first term represents the usual nearest-neighbor hopping with the transfer energy  $t = 1.6\text{eV}$ . (ii) The second term represents the spin-orbit (SO) coupling with  $\lambda_{\text{SO}} = 3.9\text{meV}$ , where  $\boldsymbol{\sigma} = (\sigma_x, \sigma_y, \sigma_z)$  is the Pauli matrix of spin, with  $\nu_{ij} = +1$  if the next-nearest-neighboring hopping is anticlockwise and  $\nu_{ij} = -1$  if it is clockwise with respect to the positive  $z$  axis. (iii) The third term represents the second Rashba SO coupling with  $\lambda_{\text{R2}} = 0.7\text{meV}$  associated with the next-nearest-neighbor hopping term, where  $t_z^i = \pm 1$  for  $i$  representing the  $A$  ( $B$ ) site, and  $\tilde{\mathbf{d}}_{ij} = \mathbf{d}_{ij} / |\mathbf{d}_{ij}|$  with the vector  $\mathbf{d}_{ij}$  connecting two sites  $i$  and  $j$  in the same sublattice. (iv) The fifth term [12] is the staggered sublattice potential term. Due to the buckled structure the two sublattice planes are separated by a distance, which we denote by  $2\ell$  with  $\ell = 0.23\text{\AA}$ . It generates a staggered sublattice potential  $\propto 2\ell E_z$  between silicon atoms at  $A$  sites and  $B$  sites in electric field  $E_z$ . (v) The fourth term represents the sublattice dependent exchange magnetization with exchange field  $M_{t_z}^i$  ( $M_A$  or  $M_B$ ). Sublattice dependence may be induced by attaching two ferromagnets from both sides of silicene.

The low-energy effective Hamiltonian derived from the tight binding model (1) is given by the Dirac theory around the  $K_\eta$  ( $K$  or  $K'$ ) point as

$$H_\eta = \hbar v_F (\eta k_x \tau_x + k_y \tau_y) + \eta \sigma_z \tau_z \lambda_{\text{SO}} - \ell E_z \tau_z + \eta \tau_z a \lambda_{\text{R2}} (k_y \sigma_x - k_x \sigma_y) + \bar{M} \sigma_z + \Delta M \sigma_z \tau_z, \quad (2)$$

where  $\tau_a$  are the Pauli matrices of the sublattice pseudospin. We have defined the mean and staggered exchange couplings,  $\bar{M} = \frac{1}{2}(M_A + M_B)$  and  $\Delta M = \frac{1}{2}(M_A - M_B)$ ,  $v_F = \frac{\sqrt{3}}{2}at$  is the Fermi velocity, and  $a = 3.86\text{\AA}$  is the lattice constant.

The coefficient of  $\tau_z$  is the mass of Dirac fermions in the Hamiltonian (2),

$$\Delta_{s_z}^\eta = \eta s_z \lambda_{\text{SO}} + s_z \Delta M - \ell E_z, \quad (3)$$

which may be positive, negative or zero. The band gap is given by  $2|\Delta_{s_z}^\eta|$ . It is intriguing that we can control it by changing the electric field  $E_z$  and the staggered exchange field  $\Delta M$ . We may make a full advantage of the spin-valley dependent Dirac mass to materialize valleytronics in silicene.

There are two types of topological phase transitions in silicene. One occurs when the Dirac mass becomes zero,  $\Delta_{s_z}^\eta = 0$ , while the other occurs when the tip of any band touches the Fermi energy. We discuss these two cases successively.

**Phase diagram in  $(E_z, \Delta M)$  plane:** We investigate the topological phase transition in the  $(E_z, \Delta M)$  plane by setting  $M_A = -M_B$ . The topological phase transition is governed solely by the Dirac mass  $\Delta_{s_z}^\eta$  given by (3). It occurs when the sign of the mass changes. The topological quantum numbers are the Chern number  $\mathcal{C}$  and spin-Chern number  $\mathcal{C}_s$  modulo 2. They are given by  $\mathcal{C} = \mathcal{C}_\uparrow^K + \mathcal{C}_\uparrow^{K'} + \mathcal{C}_\downarrow^K + \mathcal{C}_\downarrow^{K'}$ , and  $\mathcal{C}_s = \frac{1}{2}(\mathcal{C}_\uparrow^K + \mathcal{C}_\uparrow^{K'} - \mathcal{C}_\downarrow^K - \mathcal{C}_\downarrow^{K'})$ , where  $\mathcal{C}_{s_z}^\eta$  is the summation of the Berry curvature in the momentum space over all occupied

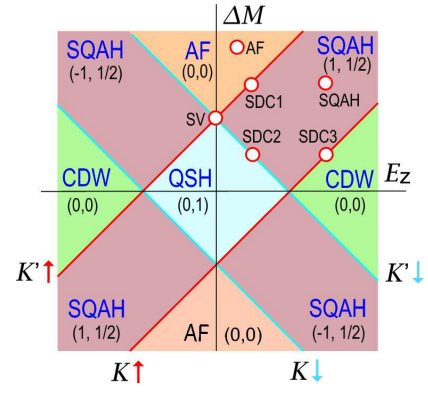


FIG. 1: (Color online) Phase diagram in the  $\ell E_z$ - $\Delta M$  plane. Heavy lines represent phase boundaries where the band gap closes. There are three types of topological insulators as indicated by QSH with  $(0, 1)$  and SQAH with  $(\pm 1, \frac{1}{2})$ . There are two types of trivial band insulators as indicated by AF and CDW. There emerge the SDC semimetal and the SV semimetal in the phase boundary. A circle shows a point where the energy spectrum is shown in Fig. 2.

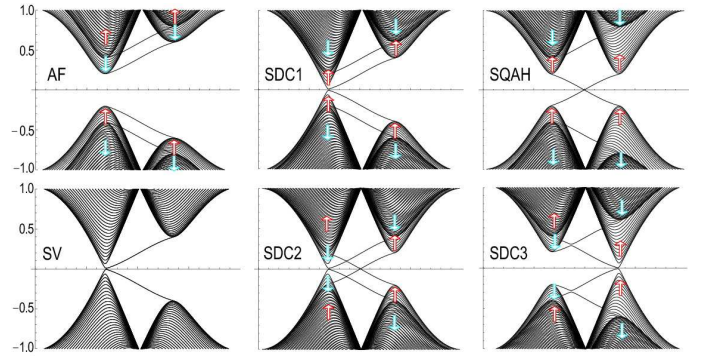


FIG. 2: (Color online) The band structures of zigzag silicene nanoribbons at the points indicated in the phase diagram [Fig. 1]. The vertical axis is the energy in unit of  $t$ , and the horizontal axis is the momentum. We can clearly see the Dirac cones representing the energy spectrum of the bulk. Lines connecting the two Dirac cones are edge modes.

states of electrons with spin  $s_z$  in the Dirac valley  $K_\eta$ . It is straightforward to calculate  $\Delta_{s_z}^\eta$ ,

$$\mathcal{C}_{s_z}^\eta = \frac{\eta}{2} \text{sgn}(\Delta_{s_z}^\eta) \quad (4)$$

as a function of the Dirac mass  $\Delta_{s_z}^\eta$ .

We present the topological phase diagram in the  $(E_z, \Delta M)$  plane. The phase boundaries are given by solving  $\Delta_{s_z}^\eta = 0$ , which yields four heavy lines corresponding to  $s_z = \uparrow\downarrow$  and  $\eta = K, K'$  in the phase diagram [Fig. 1]. The topological numbers  $(\mathcal{C}, \mathcal{C}_s)$  are calculated with the use of (4). We illustrate the spin-valley structure of topologically protected phases in Fig. 2.

First, there appear four types of insulators: (1) The spin-polarized QAH (SQAH) insulators with  $(\mathcal{C}, \mathcal{C}_s) = (\pm 1, \frac{1}{2})$ . (2) The QSH insulator with  $(0, 1)$ . (3) The trivial charge-density-wave-type (CDW) band insulator with  $(0, 0)$ . (4) The

trivial antiferromagnetic-order-type (AF) band insulator with  $(0,0)$ . We note that there are two types of trivial band insulators. The band gaps are different between the  $K$  and  $K'$  points in the AF insulator, while they are identical in the CDW insulator.

Second, SDC metals appear in the three phase boundaries of the SQAH insulator. The SDC metal is originally found in silicene by applying photo-irradiation and electric field simultaneously[13]. It is interesting that the SDC state is also obtainable without photo-irradiation. On the other hand, the SV semimetal appears at the point where the four topological insulators meet. They are topologically protected semimetals, since they appear in the interface of different topological insulators each of which is topologically protected against small perturbations.

We may apply an inhomogeneous electric field[12]  $E_z(x, y)$  or generate a domain wall in the antiferromagnet  $\Delta M(x, y)$ , which makes the Dirac mass inhomogeneous. For simplicity we assume the homogeneity in the  $x$  direction. The zero modes appear along the line determined by  $\Delta_{s_z}^\eta(y) = 0$ , when  $\Delta_{s_z}^\eta(y)$  changes the sign. We may set  $k_x = \text{constant}$  due to the translational invariance along the  $x$  axis. We seek the zero-energy solution. The particle-hole symmetry guarantees the existence of zero-energy solutions satisfying the relation  $\psi_B = i\xi\psi_A$  with  $\xi = \pm 1$ . Here,  $\psi_A$  is a two-component amplitude with the up spin and down spin. Setting  $\psi_A(x, y) = e^{ik_x x} \phi_A(y)$ , we obtain  $H_\eta \psi_A(x, y) = E_{\eta\xi} \psi_A(x, y)$ , together with a linear dispersion relation  $E_{\eta\xi} = \eta\xi \hbar v_F k_x$ . We can explicitly solve this as

$$\phi_{As_z}(y) = C \exp \left[ \frac{\xi}{\hbar v_F} \int^y \Delta_{s_z}^\eta(y') dy' \right], \quad (5)$$

where  $C$  is the normalization constant. The sign  $\xi$  is determined so as to make the wave function finite in the limit  $|y| \rightarrow \infty$ . This is a reminiscence of the Jackiw-Rebbi mode[28] presented for the chiral mode. The difference is the presence of the spin and valley indices in the wave function.

**Phase diagram in  $(M_A, M_B)$  plane:** We proceed to derive the topological phase diagram in the  $(M_A, M_B)$  plane by setting  $E_z = 0$ , and make its physical interpretation. We present our result in Fig.3, where the phase boundaries are not determined by the condition  $\Delta_{s_z}^\eta = 0$ . This condition gives two dotted lines in the phase diagram [Fig.3]. We show soon how to derive the phase boundaries. We have also calculated the band structure of a silicene nanoribbon with zigzag edges, which we give in Fig.4 for typical points in the phase diagram.

Diagonalizing the Hamiltonian (2) we obtain four energy levels,

$$E_{s_z}^\eta = \pm \sqrt{(a\lambda_R k)^2 + F_\pm(k)^2}, \quad (6)$$

with  $F_\pm(k) = \eta s_z \bar{M} \pm \sqrt{(\hbar v_F k)^2 + (\eta \lambda_{SO} + \Delta M)^2}$ . When two energy levels coincide, the band gap becomes zero. This occurs at the  $K$  and  $K'$  points, where  $k_\pm = 0$ . The band closes when  $\Delta M = -\eta \lambda_{SO}$  for the  $K_\eta$  point.

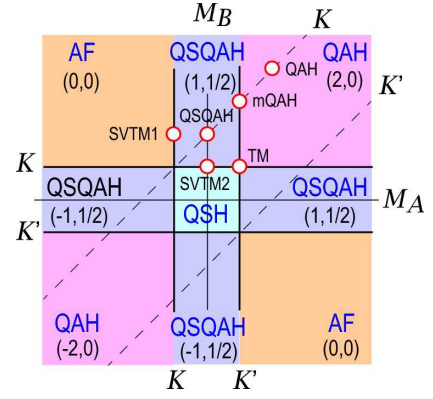


FIG. 3: (Color online) Phase diagram in the  $M_A$ - $M_B$  plane. Dotted lines represent the points where the band gap closes. Heavy lines represent phase boundaries. There are five types of topological insulators as indicated by QAH with  $(\pm 2, 0)$ , QSQA with  $(\pm 1, 1/2)$  and QSH with  $(0, 1)$ . There is one trivial band insulator as indicated by AF. There emerge the mQAH metal and the TM in the phase boundary. A circle shows a point where the energy spectrum is calculated and shown in Fig.4.

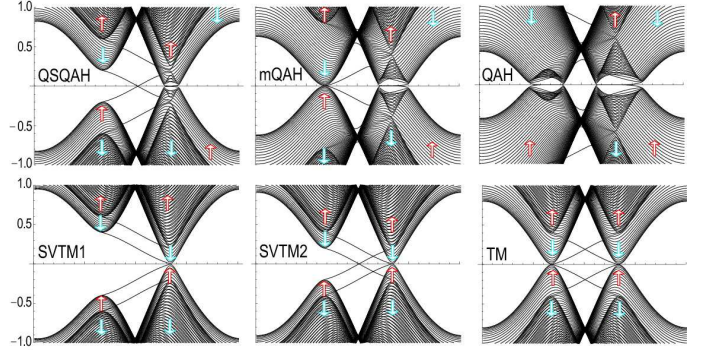


FIG. 4: (Color online) The band structure of a silicene nanoribbon at marked points in the phase diagram [Fig.3]. The vertical axis is the energy in unit of  $t$ , and the horizontal axis is the momentum. Lines connecting the two Dirac cones are edge modes.

We determine the phase boundary. It is determined by the condition that the tip of any band touches the Fermi energy. Silicene is a metal on the phase boundary. The energy spectrum at  $k = 0$  is given by

$$E_{s_z, t_z}^\eta = \eta s_z t_z \lambda_{SO} + \bar{M} s_z + \Delta M s_z t_z. \quad (7)$$

It vanishes when  $M_A = -\lambda_{SO}$  or  $M_B = \lambda_{SO}$  for the  $K$  point, and  $M_A = \lambda_{SO}$  or  $M_B = -\lambda_{SO}$  for the  $K'$  point.

The topological numbers are  $\mathcal{C} = \mathcal{C}^K + \mathcal{C}^{K'}$  and  $\mathcal{C}_s = \mathcal{C}_s^K + \mathcal{C}_s^{K'}$ , where  $\mathcal{C}^\eta = \mathcal{C}_A^\eta + \mathcal{C}_B^\eta$  and  $\mathcal{C}_s^\eta = \frac{1}{2}\eta(\mathcal{C}_A^\eta - \mathcal{C}_B^\eta)$  with

$$\mathcal{C}_{t_z}^\eta = \frac{1}{2} \text{sgn}(\eta t_z \lambda_{SO} + M_{t_z}). \quad (8)$$

We illustrate the spin-valley structure of typical states in Fig.4.

First, there appear four types of insulators: (1) The QSQA insulators with  $(\mathcal{C}, \mathcal{C}_s) = (\pm 1, 1/2)$ , where the QAH effect

is realized at one valley in coexistence with the QSH effect at the other valley. It is intriguing that, e.g., the topological numbers  $(\pm 1, 0)$  are assigned to the  $K$  point and  $(0, 1/2)$  to the  $K'$  point. (2) The trivial AF insulator with  $(0, 0)$ . (3) The QSH insulator with  $(0, 1)$ . (4) The QAH phases with  $(2, 0)$  for  $M > 0$  and  $(-2, 0)$  for  $M < 0$ .

Second, at the boundary, the topological metal (TM) and the single-valley topological metal (SVTM) emerge. The band touches parabolically in them. Their emergencies are also protected topologically since they are sandwiched by different topological insulators.

**Optical absorption:** An interesting experiment to probe and manipulate the valley degree of freedom is optical absorption[3–7, 27]. We briefly discuss that spin-valley dependent band structures we have found will be experimentally observable by spin-valley-selective circular dichroism. Circular dichroism is a phenomena in which the response of the left- and right-handed circularly polarized light is different. To assess the optical selectivity of spin and valley by circularly polarized light, we compute the spin-valley dependent degree of circular polarization, between the top valence bands and bottom of conduction bands. If we neglect the Rashba terms ( $\lambda_{R2} = 0$ ) we are able to obtain an analytic formula for the transitions near the  $K_\eta$  point,

$$|P_{\pm}^{\eta}(k)|^2 = m_0^2 v_F^2 \left( 1 \pm \eta \frac{\Delta_{s_z}^{\eta}}{\sqrt{(\Delta_{s_z}^{\eta})^2 + 4a^2 t^2 k^2}} \right)^2, \quad (9)$$

where  $P_{\pm}^{\eta}(k)$  are the interband matrix elements of the left- and right-polarized radiation fields for spin  $s_z$  at  $k$ , respectively, defined for a vertical transition from band  $u_c$  to band  $u_v$ , as  $P_{\pm}^{\eta}(k) \equiv m_0 \langle u_c(k) | \frac{1}{\hbar} \frac{\partial H_{\eta}}{\partial k_{\pm}} | u_v(k) \rangle$ . Especially we find the spin-valley dependent optical selection rule at  $k = 0$ ,

$$|P_{\pm}^{\eta}(0)|^2 = m_0^2 v_F^2 (1 \pm \eta \text{sgn}(\Delta_{s_z}^{\eta}))^2, \quad (10)$$

which will be detected experimentally. Such a spin-valley selective circular dichroism would lead to the eventual realization of spin-valleytronics.

In this paper, making the use of the buckled structure, we have shown that we are able to make a full control of the spin and valley degrees of freedom in silicene. The emergence of a relevant state with a particular spin-valley structure is topologically protected. In exploring the phase diagram, we have found a hybrid topological insulator named Quantum-Spin-Quantum-Anomalous Hall (QSQAH) insulator, where two different topological insulators coexist: The QSH effect is realized at one valley while the QAH effect is realized at the other valley. The topological numbers are simply given by one half of the sum of those of the QSH and QAH insula-

tors. Such a hybrid of two distinctive topological insulators is utterly a new state.

I am very much grateful to N. Nagaosa for many fruitful discussions on the subject. This work was supported in part by Grants-in-Aid for Scientific Research from the Ministry of Education, Science, Sports and Culture No. 22740196.

- 
- [1] A. Rycerz, J. Tworzydło, and C. W. J. Beenakker, *Nat. Phys.* **3**, 172 (2007).
  - [2] D. Xiao, W. Yao, and Q. Niu, *Phys. Rev. Lett.* **99**, 236809 (2007).
  - [3] W. Yao, D. Xiao, and Q. Niu, *Phys. Rev. B* **77**, 235406 (2008).
  - [4] D. Xiao, G.-B. Liu, W. Feng, X. Xu, and W. Yao, *Phys. Rev. Lett.* **108**, 196802 (2012).
  - [5] H. Zeng, J. Dai, W. Yao, D. Xiao and X. Cui, *Nat. Nanotech.* **7**, 490 (2012).
  - [6] T. Cao, G. Wang, W. Han, H. Ye, C. Zhu, J. Shi, Q. Niu, P. Tan, E. Wang, B. Liu and J Feng *Nat. Com.* **3**, 887 (2012).
  - [7] X. Li, T. Cao, Q. Niu, J. Shi, and J Feng, *cond-mat/arXiv:1210.4623*
  - [8] P. Vogt, P. De Padova, C. Quaresima, J. A., E. Frantzeskakis, M. C. Asensio, A. Resta, B. Ealet and G. L. Lay, *Phys. Rev. Lett.* **108**, 155501 (2012).
  - [9] C.-L. Lin, R. Arafune, K. Kawahara, N. Tsukahara, E. Minamitani, Y. Kim, N. Takagi, M. Kawai, *Appl. Phys. Express* **5**, 045802 (2012).
  - [10] A. Fleurence, R. Friedlein, T. Ozaki, H. Kawai, Y. Wang, and Y. Yamada-Takamura, *Phys. Rev. Lett.* **108**, 245501 (2012).
  - [11] C.-C. Liu, W. Feng, and Y. Yao, *Phys. Rev. Lett.* **107**, 076802 (2011).
  - [12] M. Ezawa, *New J. Phys.* **14**, 033003 (2012).
  - [13] M. Ezawa, *cond-mat/arXiv:1207.6694* (to be published in *Phys. Rev. Lett.*)
  - [14] M. Ezawa, *Phys. Rev. Lett* **109**, 055502 (2012).
  - [15] C. L. Kane and E. J. Mele, *Phys. Rev. Lett.* **95**, 226801 (2005).
  - [16] M. Onoda and N. Nagaosa, *Phys. Rev. Lett.* **90**, 206601 (2003).
  - [17] Z. Qiao, S. A. Yang, W. Feng, W-K. Tse, J. Ding, Y. Yao, J. Wang, and Q. Niu, *Phys. Rev. B* **82**, 161414 R (2010).
  - [18] W.-K. Tse, Z. Qiao, Y. Yao, A. H. MacDonald, and Q. Niu, *Phys. Rev. B* **83**, 155447 (2011).
  - [19] J. Ding, Z. Qiao, W. Feng, Y. Yao and Q. Niu, *Phys. Rev. B* **84**, 195444 (2011).
  - [20] Z. Qiao, H. Jiang, X. Li, Y. Yao and Q. Niu, *Phys. Rev. B* **85**, 115439 (2012).
  - [21] C.-X. Liu, X.-L. Qi, X. Dai, Z. Fang and S.-C. Zhang, *Phys. Rev. Lett.* **101**, 146802 (2008).
  - [22] M.Z Hasan and C. Kane, *Rev. Mod. Phys.* **82**, 3045 (2010).
  - [23] X.-L. Qi and S.-C. Zhang, *Rev. Mod. Phys.* **83**, 1057 (2011).
  - [24] C. Wu, B.A. Bernevig and S.-C. Zhang, *Phys. Rev. Lett.* **96**, 106401 (2006).
  - [25] H. B. Nielsen and M. Ninomiya, *Nucl. Phys. B* **185**, 20 (1981).
  - [26] C.-C. Liu, H. Jiang, and Y. Yao, *Phys. Rev. B*, **84**, 195430 (2011).
  - [27] M. Ezawa, *Phys. Rev. B* **86**, 161407(R) (2012).
  - [28] R. Jackiw and C. Rebbi, *Phys. Rev. D* **13**, 3398 (1976).